Eng. Sci., 2020, 11, 19-30

Engineered Science

DOI: https://dx.doi.org/10.30919/es8d1128

Recent Advances in Co_3O_4 as Anode Materials for High-Performance Lithium-Ion Batteries

Chuanxin Hou,[1] Bing Wang,[2] Vignesh Murugadoss,[3,4] Sravanthi Vupputuri,[3] Yunfeng Chao,[5] Zhanhu Guo,[3,*] Caiyun Wang[5,*] and Wei Du[1,*]

Abstract

Lithium ion batteries (LIBs) have been widely applied as energy storage devices for large-scale electrical vehicle markets. Designing and ameliorating new or existing anodes are in high demand to meet the requirements of the next generation LIBs with higher energy/power densities, more excellent rate capability and longer cycling performance. Co_3O_4-based materials have drawn great attention as potential alternatives to the current graphite anodes due to the high capacity, abundant reserves of resource, moderate price, and simple preparation process. However, their inherent shortcoming of low conductivity and huge volume changes limit the practical applications. Different approaches have been applied to overcome these drawbacks. Herein, we summarize the recent developments in high-performance Co_3O_4anode materials from their architectures, including 0D nanostructures (nanospheres, nanocrystals, nanoparticles, nanocages and nanocubes), 1D nanostructures (nanowires, nanofibers, nanorods and nanotubes), 2D nanostructures (nanosheets, nanofoils, nanoflakes and nanofilms), and 3D structures (microsized cages, hollow structures, mesoporous structure, flower-like structure). We expect that this review will shed light on the structure-property relationship for rational design and synthesis of Co_3O_4-based materials and promote the practical application.

Keywords: Co_3O_4; Anode; Composites; Nanostructure; Li-ion Batteries.
Received: 7 June 2020; Accepted: 22 July 2020.
Article type: Review article.

1. Introduction

Currently, enormous efforts have concentrated on the exploitation of new energy storage to effectively use intermittent renewable energy for replacing traditional non-renewable energy sources, which cause increasingly serious environmental problems such as acid rain, smog, greenhouses effect and so on.[1-6] Lithium ion batteries (LIBs) are dominating the present battery market due to the high energy density, wide operation temperature range, rapid charge/discharge capability, long cycle life and no memory effect.[7-9]

Rechargeable LIBs are regarded as one of the most successful energy storage devices since the first commercial application by Sony Corporation.[8,10] LIBs consist of three main components: anode electrodes, cathode electrodes and electrolyte. Anode and cathode electrodes are separated by polypropylene film that is saturated with electrolyte. Nowadays, $LiMn_2O_4$, $LiNiO_2$, $LiCoO_2$, $LiFePO_4$, and Lithium-rich layered xLi_2MnO_3-$(1-x)LiNi_{1/3}Co_{1/3}Mn_{1/3}$ materials have been widely used as cathode electrodes in commercial LIBs.[11-13] However, the mature anode materials are only limited to graphite materials including silicon/graphite composite containing no more than 15% Si, due to its merits of excellent cycling performance, inexpensive and relatively low working voltage*vs.* Li/Li^+.[14] A schematic illustration of a working LIB based on a $LiCoO_2$ cathode and a graphite anode is shown in Fig. 1. During the charging process, Li ions are de-intercalated from $LiCoO_2$

[1] *School of Environmental and Material Engineering, Yantai University, No. 30 Qingquan Road, Yantai, Shandong, 264005, China.*
[2] *Key Laboratory for Biomedical Effects of Nanomaterials and Nanosafety, Institute of High Energy Physics, Chinese Academy of Sciences, Beijing 100049, China.*
[3] *Integrated Composites Laboratory (ICL), Department of Chemical & Biomolecular Engineering, University of Tennessee, Knoxville, TN 37996, USA.*
[4] *Electrochemical Energy Research Lab, Centre for Nanoscience and Technology, Pondicherry University, Puducherry, 605 014, India.*
[5] *ARC Centre of Excellence for Electromaterials Science, Intelligent Polymer Research Institute, AIIM Facility, University of Wollongong, North Wollongong, NSW 2500, Australia.*
**E-mail: caiyun@uow.edu.au (C. Wang); zguo10@utk.edu (Z. Guo); duwei@ytu.edu.cn (W. Du).*

electrode and travel towards to graphite anode across polypropylene film through the electrolyte, and then insert into graphite electrode; at the same time, the electrons move to anode side from cathode side through the external circuit in order to maintain the electrical neutrality of the material. Vice versa, Li ions are de-intercalated from the graphite electrode and move back to the $LiCoO_2$ cathode during the discharge process, and electrons move back to the cathode side from the anode side. The efficient conversion of chemical energy to electric energy inside a lithium-ion battery is implemented by the de-intercalation/intercalation processes of Li^+ accompanied with an equal charge quantity of electron transfer. The electrochemical reactions can be described by the following Equations:

Anode:

$$xLi^+ + 6C + xe^- \leftrightarrow Li_xC_6 \quad (1)$$

Cathode:

$$LiCoO_2 \leftrightarrow Li_{1-x}CoO_2 + xLi^+ + xe^- \quad (2)$$

Overall reaction:

$$LiCoO_2 + 6C \leftrightarrow Li_{1-x}CoO_2 + Li_xC_6 \quad (3)$$

Currently, LIBs are dominantly used in portable electronics, the ever-growing applications that need high energy/power capacities, such as high-power electric vehicles, large spacecraft and national grid, etc. They place greater demands on LIBs with better electrochemical behaviors, which depend on the breakthroughs in electrode materials.[15]

2. Overview of Anode Electrodes

The conventional graphite offers a relatively low theoretical capacity of 372 mAh g^{-1}.[14] Therefore, different carbon based and non-carbon based materials with higher lithium storage capacity have been exploited, as shown in Fig. 2. Carbon-based materials include, but are not limited to, graphene, amorphous carbon, carbon nanotubes, and carbon nanofibers.[14] Non-carbon materials mainly include lithium metal, silicon, titanium dioxide, germanium, transition metal oxides, transition metal nitride, transition metal sulfide, transition metal phosphides, and transition metal carbides.[16]

The state-of-art anodes materials are classified into three categories according to the electrochemical lithiation/delithiation mechanism as shown in Fig. 3. One type is alloy anodes based on an alloying/dealloying reaction ($M+ xLi^+ \leftrightarrow Li_xM$), which mainly contain silicon, germanium, silicon monoxide, and stannic oxide; This family materials exhibit high energy density, higher specific capacity and good safety, but with huge volume changes during cycling processes, resulting in capacity fading and poor cycling performance.[17] The second type is intercalation anodes based on the lithium insertion/extraction mechanism($MX_2+ Li^+ \leftrightarrow LiMX_2$), which mainly include carbon based materials, titanium dioxide, $Li_4Ti_5O_{12}$, and niobium pentoxide; They usually present good working potential, long cycle lifespan and low price, but with relatively low capacity and low energy density. The third type is conversion anodes based on the redox reaction mechanism ($MX+ 2Li^+ \leftrightarrow Li_2X+ M$), which is most commonly referred to transition metal oxides, nitride, sulfide, phosphides, carbides, etc. They commonly show high specific capacity and low operation potential, but with relatively low coulombic efficiency, poor cycling lifespan and unstable SEI.[17,18]

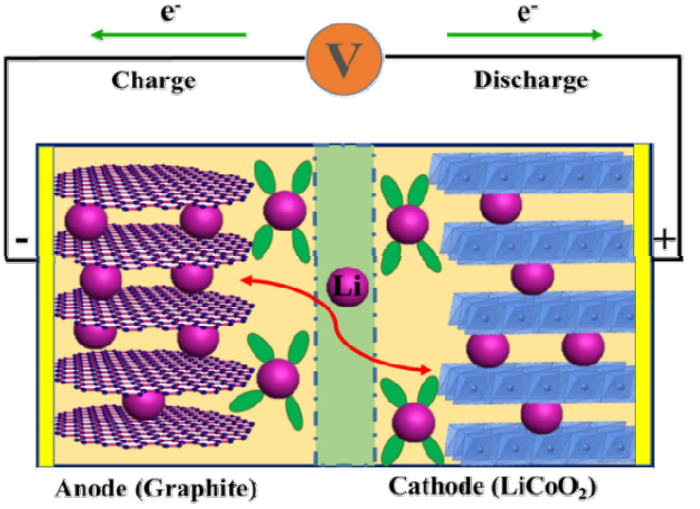

Fig. 1 Schematic illustration of a typical LIB (cathode: $LiCoO_2$; anode: graphite).

All the mentioned three types of anode electrodes have shown huge application potential for the next generation LIBs. The intercalation anodes show good electrochemical properties of long-cycling life, low price, low working potential, and extreme safety during charge/discharge processes. However, this type of anodes also shows the relatively low capacity and low density compared with alloy and conversion anodes.[18-20] The alloy anodes, such as Si material, show superior high capacity (4200 mAh g^{-1}) and high energy density. However, this kind of anodes presents large irreversible capacity, huge volume changes during cycling (Si, 400 %), which cause the huge capacity fading and poor cycle life performance compared with intercalation and conversion anodes.[17-20] The conversion anodes own relatively higher theoretical capacity compared with intercalation anodes, and relatively low volume changes during the cycling compared with alloy anodes. In addition, these anodes show the merits of environmental benignity and low cost, attracting more and more attention as the substitute for the current anode material graphite of the next generation LIBs.[21]

Recently, transition metal oxides, as a kind of conversion anodes, including MnO, SnO_2, MnO_2, Fe_3O_4, Fe_2O_3, NiO, etc., are becoming the star anodes for LIBs, due to the high capacity, large reserves, low cost and environment-friendliness.[22] Among various electrode materials, Co_3O_4 has been investigated for many years in

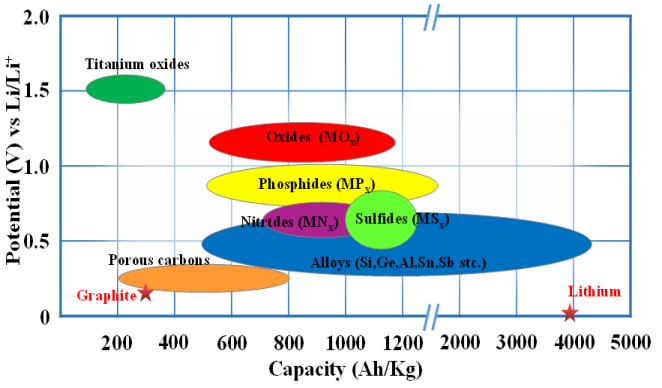

Fig. 2 Schematic illustration of anode electrodes for the LIBs.

virtue of its advantages of high theoretical specific capacity (890 mAh g^{-1}), wide availability, easy preparation and stable chemical properties since its first applied as the anode electrode for LIBs by Poizot at 2000.[23,24]More than 1000 papers about Co_3O_4-based electrodes for LIBs have been published in the last 5 years according to the database of Web of Science, confirming the continued hot attention. More and more works were carried out to obtain the capacity higher than the theoretical specific capacity of Co_3O_4, better rate capability and longer cycling performance due to the unique designed nanostructures. Here, we will present the recent advances in rationally designed nanostructures of high performance Co_3O_4-based anodes that focus on the illustration of structure-property relationship. We will also present our perspectives on the methods to enhance the electrochemical performance of nanostructured Co_3O_4-based anodes for the new generation of LIBs.

3. Nanostructured high-performance Co_3O_4-based Anodes

Despite that Co_3O_4-based anodes are considered as the star materials for LIBs anode, they still suffer from some drawbacks including relatively low electronic conductivity and huge volume changes during the intercalation/deintercalation of Li^+, impeding the practical application. Constructing different nanostructures for Co_3O_4 electrodes is an efficient strategy to solve the mentioned problems and enhance the electrochemical performance due to the shortened Li^+ transport path, increased specific surface area and increased number of active sites.[18,25] As a consequence, different morphologies of Co_3O_4 electrodes have been developed, including zero dimensional material, one dimensional material, two dimensional materials and three dimensional materials.

3.1 Zero Dimensional Co_3O_4-based Anodes

Zero Dimensional (0D) nanostructures usually refer to the particles at the nano scale with some special characters.[26,27] The 0D Co_3O_4-based materials include nanospheres, nanocrystals, nanoparticles, nanocages and nanocubes (Fig. 4), which can offer more active sites, shorten transport pathways, increase the contact area between electrolyte and electrode, and promote the intercalation/deintercalation of Li^+ process. Thus, the electrochemical performance of Co_3O_4-based electrodes has been greatly improved.

Chen *et al*. prepared Co_3O_4 nanocages by heat treatment of cobalt-based Prussian blue analogues. The obtained unique designed nanocages samples showed large specific surface area, resulting in excellent electrochemical performance. They confirmed that the better crystallinity, moderate particle size and multihole structure of samples enhanced the electrochemical properties of initial coulomb efficiency and cycle stability.[28] In Xiao's research (Fig 4a), single-crystalline Co_3O_4 cubes have been successfully obtained via a simple hydrothermal method, which displayed a discharge capacity of 877 mAh g^{-1} at 0.2 A g^{-1} after 110 cycle-life.[29] Kim *et al* prepared Co_3O_4 nanoparticles and obtained a reversible capacity of ~1100 mAh g^{-1} at 1.0 A g^{-1} after 150 cycles.[30]

In order to further improve the electrochemical performance of Co_3O_4-based electrodes, conductive carbon[39] as additives or supports have been introduced such as carbon nanotubes,[31] porous carbon,[32] graphene oxide.[40] The choice of carbon materials is based on the following merits. First, conductive carbon additives themselves have been widely applied as electrodes for energy storage devices due to its advantages of giveaway prices, good chemical and physical stability, relatively high capacity, high conductivity, and light weight.[41] Second, conductive carbon additives can effectively alleviate volume changes during cycling performance.[21] Han *et al*. has shown that the compounds of Co_3O_4 nanoparticles and porous carbon nanotube sponge obtained by intense densification, which light up a high efficiency and inexpensive method to develop high areal capacity and high mass loading electrodes for LIBs[31] (Fig 4b).

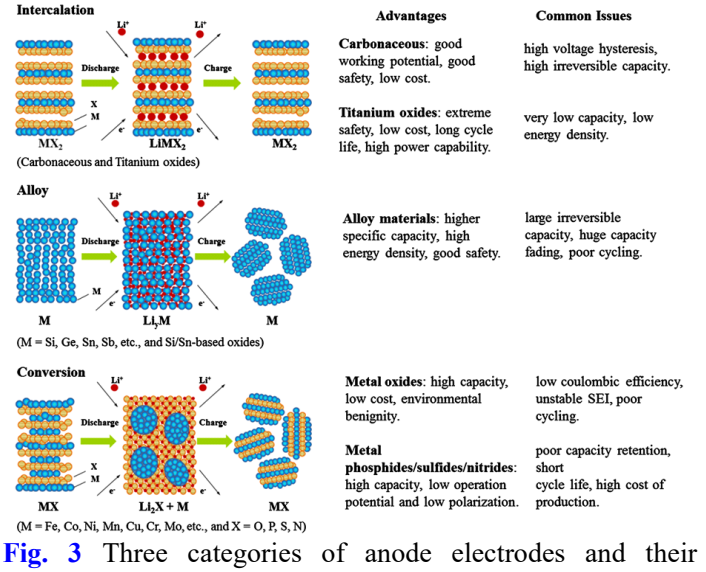

Fig. 3 Three categories of anode electrodes and their characteristics. Reproduced with permission.[17] Copyright 2018, Springer.

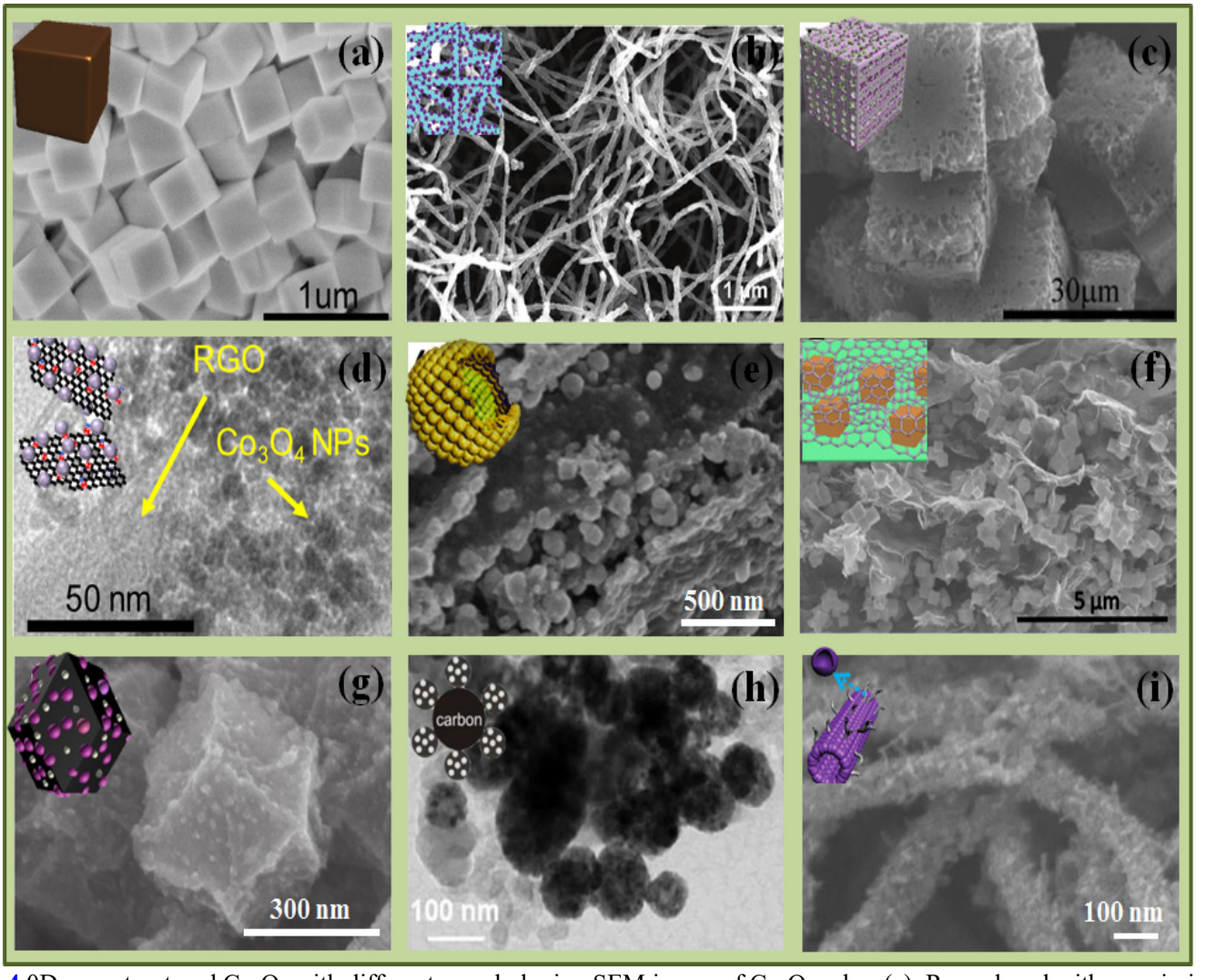

Fig. 4 0D nanostructured Co_3O_4 with different morphologies: SEM image of Co_3O_4 cubes (a), Reproduced with permission.[29] Copyright 2018, Springer. SEM image of Co_3O_4-CNT nanocomposites (b), Reproduced with permission.[31] Copyright 2018, WILEY-VCH. SEM image of Co_3O_4 nanoparticles@C cube (c), Reproduced with permission.[32] Copyright 2018, Elsevier. TEM image of Co_3O_4 /graphene composites (d), Reproduced with permission.[33] Copyright 2017, Elsevier. SEM image of Co_3O_4 nanospheres@N-C framework (e), Reproduced with permission.[34] Copyright 2016, American Chemical Society. SEM image of sandwich-shape Co_3O_4/Graphene composites (f), Reproduced with permission.[35] Copyright 2017, American Chemical Society. SEM image of Co_3O_4/Co/carbon nanocages (g), Reproduced with permission.[36] Copyright 2017, Elsevier. TEM image of hollow Co_3O_4 nanoparticles (h), Reproduced with permission.[37] Copyright 2015, American Chemical Society. SEM image of Co_3O_4 nanoparticles/Carbon nanotube (i), Reproduced with permission.[38] Copyright 2016, Wiley-VCH.

Wang *et al.* reported one strategy to load Co_3O_4 nanoparticles on MOF-5-derived porous carbon, and the composites exhibited high capacity at high current density and superior exceptional rate capability[32] (Fig 4c). Meanwhile, Wang's group prepared multi-walled carbon nanotubes/Co_3O_4 nanocomposites that were inserted into metal organic frameworks and obtained outstanding electrochemical performance as anodes for LIBs.[42] Ham *et al.* reported a shape-controlled synthesis of Co_3O_4 nanoparticles of less than 10 nm that were dispersed in reduced graphene oxide, and the prepared composites showed a distinguished capacity of 1600 mAh g^{-1} at 0.05 A g^{-1} after 100 cycles[33] (Fig 4d). The composites obtained from the loading of single yolk-shell-structured Co_3O_4@Co_3O_4 nanospheres into the N-doped carbon framework delivered enviable high capacity and desired rate capability[34] (Fig 4e). A heterostructure structure was introduced between Co_3O_4 nanoparticles and carbon nanotubes by Song *et al.* with improved rate capability, capacity and cycling performance.[43] Besides, a sandwich-like structure that consists of Co_3O_4 nanocubes and graphene sheets was formed and the relationship of the excellent electrochemical performance and the unique structure were explored via *in situ* electrochemical XRD[35] (Fig 4f). The co-incorporation of metallic Co and conductive carbon materials into the Co_3O_4 nanostructures could further improve the electrochemical performance[36,44,45] (Fig 4g).

In addition, building up hollow structure or mesoporous structure has been proved to improve the electrochemical performance of nanosized Co_3O_4 electrodes. Wang *et al.* reported hollow Co_3O_4 nanoparticles supported by carbon matrix prepared by a method of impregnation-reduction coupled with the following oxidation process in air atmosphere. The composites exhibited superior electrochemical performance, thanks to the unique hollow structure that benefits the transportation of electrons and Li^+ as well as buffers the stress caused by the huge volume changes during the cycling process, as shown in Fig 1h[37] (Fig 4h). The composites consisting of hollow Co_3O_4 nanoparticles and carbon nanotubes were reported by Lou's group. The as-prepared composites delivered a high capacity of 1281 mAh g^{-1} at 0.1 A g^{-1} after 200 cycles due to the merits of the distinctive structures, including that the hollow structure offered more active sites, enhanced structural stability, and the carbon nanotubes improved the conductivity of electrons and effective inhibition of particle aggregation[38] (Fig 4i).

3.2 One Dimensional Co_3O_4-based Anodes

One Dimensional (1D) nanostructures usually refer to nanowires, nanofibers, nanorods and nanotubes.[46-51] The 1D nanostructures have been extensively used in the field of energy storage on account of the characteristics of shortened electrons and ions transmission pathway, more active sites, increased contact area between electrodes and electrolyte. For Co_3O_4-based materials, the 1D nanostructures can also restrain the volume changes during the intercalation/deintercalation process of Li^+ and limit the agglomeration of nanoparticles[52] (Fig 5a).

Chen *et al.* synthesized hollow Co_3O_4 fibers by the method of chemical precipitation and thermal decomposition and the as-prepared samples showed high capacity of 1177.4 mAh g^{-1} at 0.1 A g^{-1} and a relatively high initial coulombic efficiency of 82.9 %. The enhanced electrochemical performance was ascribed to the unique 1 D structure that increased the specific surface area to offer more active sites and contact area and the void space to accommodate the volume change during cycling[53] (Fig 5b). Zhang' group distributed Co_3O_4hollow nanoparticles onto porous carbon fiber to form the 1 D structure, and the composite exhibited a high reversible capacity of 1100 mAh g^{-1} at 0.1 A g^{-1} after 200 cycle-life[54] (Fig 5c). The Co_3O_4nanofibers were also prepared by electrospinning technology and showed outstanding capacity and cycling performance[55] (Fig 5d). Yan *et al.* reported carbon-doped Co_3O_4hollow nanofibers and obtained superior performance, the structure-property relationship was evidenced by density functional theory (DFT) calculations[56] (Fig 5e). The Co_3O_4nanofibers can also be synthesized by the hydrothermal method[57,64] (Fig 5f), template-based engineering[65] and hydrolysis strategy[58] (Fig 5g), and all the as-prepared samples delivered outstanding electrochemical performance.

In addition to nanofibers, Co_3O_4 nanotubes and nanorods have also been developed as anode electrodes for LIBs. Co_3O_4@Carbon nanotube arrays were synthesized by Zhao's group and showed desirable performance in capacity, rate capability and cycle stability.[52] The formation mechanism of Co_3O_4mesoporous nanotubes was controlled by releasing of the gas originated from organic oxidation reaction and kokendar effect and the electrochemical performance were enhanced[59] (Fig 5h). The Co_3O_4 hollow nanotubes were synthesized by Yan *et al*. They introduced the concept of the local built-in electric field, causing the imbalance of charge distribution due to the C-doping, promoting the Li^+ imbedding and deblocking process, to obtain high lithium storage properties[60] (Fig 5i). The compounds of Co_3O_4 and carbon nanotubes in a hierarchically porous structure were prepared by Li and colleagues, and this distinctive structure exhibited a high reversible capacity of 1083 mAh g^{-1} at 0.5 mA g^{-1} after 140 cycles, excellent rate capability of 521mAh g^{-1} at 8.0 A g^{-1} and superior cycle stability at 1.0 A g^{-1} for 200 cycles[61] (Fig 5j).

Besides the mentioned 1D nanostructures, the Co_3O_4 nanowires were also used as LIBs anodes.[66] Mesoporous Co_3O_4 nanowires on the nickel foam were formed by the decomposition of a metal-organic framework structure, and these composites possessed a high reversible capacity of 1609 mAh g^{-1} at 0.5 A g^{-1} and excellent rate capability without the use of conductive additives. This unique structure offered more active sites, shortened the pathway for Li^+ and electrons and promoted the rapid transmission of electrons[62] (Fig 5k). Wu *et al*. reported Co_3O_4/α-Fe_2O_3 nanowire heterostructure structure, theseCo_3O_4 nanowire arrays were grown on the Ti matrix that promoted the transmission of electrons, and the α-Fe_2O_3 improved the capacity, relieved the volume changes and inhibited the aggregation of Co_3O_4 electrodes, resulting in outstanding electrochemical performance[63] (Fig 5l).

3.3 Two Dimensional Co_3O_4-based Anodes

Generally, Two Dimensional (2D) nanostructures usually refer to nanosheets, nanofoils, nanoflakes and films.[67-70] The electrons can move rapidly in the 2D nanostructures and are almost unrestricted between layers, thus accelerating reaction kinetics of electrodes for good rate capability and cycle stability.

Zhao *et al.* reported porous Co_3O_4 films that were tightly attached to Ti nanowire arrays as anode electrodes for LIBs. The as-prepared samples showed a highly desirable cycle stability of *ca.* 400 mAh g^{-1} at 20.0 A g^{-1} after 2000 cycles without significant decline.[71] Meanwhile, a kind of graphene-like, porous 2D Co_3O_4 nanofoils was synthesized and the as-prepared composites exhibited a high capacity far beyond its theoretical capacity[72] (Fig 6a).

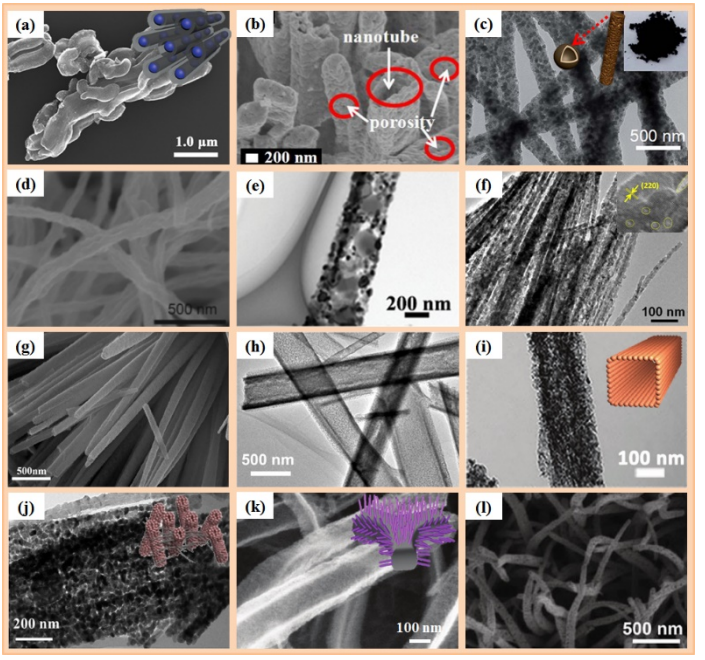

Fig. 5 1D nanostructured Co_3O_4 with different morphologies: SEM image of Peapod-like Co_3O_4@C nanotube (a), Reproduced with permission.[52] Copyright 2015, WILEY-VCH. SEM image of microfibers (b), Reproduced with permission.[53] Copyright 2017, Elsevier. TEM image of porous fibers (c), Reproduced with permission.[54] Copyright 2018, Royal Society of Chemistry. SEM image of Co_3O_4 Nanofiber (d), Reproduced with permission.[55] Copyright 2017, American Chemical Society. TEM image of Co_3O_4 hollow nanofibers (e), Reproduced with permission.[56] Copyright 2016, WILEY-VCH. TEM image of Co_3O_4 crystal nanofibers (f), Reproduced with permission.[57] Copyright 2016, Springer Nature Limited. SEM image of Co_3O_4@TiO_2 core-shell nanofibers (g), Reproduced with permission.[58] Copyright 2017, Elsevier. TEM image of Co_3O_4 mesoporous nanotubes (h), Reproduced with permission.[59] Copyright 2016, WILEY-VCH. TEM image of Co_3O_4 hollow nanotubes (i), Reproduced with permission.[60] Copyright 2018, WILEY-VCH. TEM image of Co_3O_4 nanorods/carbon nanotubes (j), Reproduced with permission.[61] Copyright 2018, WILEY-VCH. SEM image of Co_3O_4 nanowires (k), Reproduced with permission.[62] Copyright 2018, WILEY-VCH. SEM image of Co_3O_4 nanowires (l), Reproduced with permission.[63] Copyright 2013, Tsinghua University Press and Springer.

Nulu *et al*. prepared hierarchical Co_3O_4 nanoflakes arrays, which presented superior anode performance based on the rate capability and lifespan[73] (Fig 6b). Du' group reported the porous Co_3O_4 nanoplates/graphene composites, which the evolution process of the composites electrode was investigated by *in situ* TEM, found that the volume changes during cycling performance were smaller than the theoretical volume expansion due to the unique nanoplates structure, giving reasons for the stable cycling performance and high reversible capacity[74] (Fig 6c).

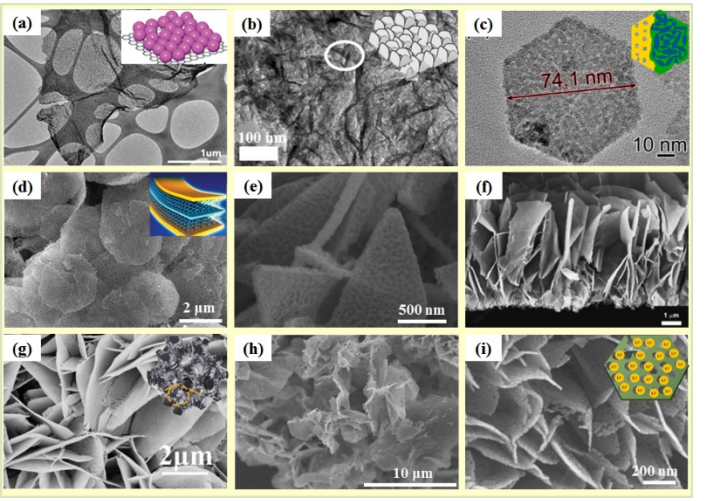

Fig. 6 2D nanostructured Co_3O_4 with different morphologies: TEM image of the 2D Co_3O_4 nanofoils (a), Reproduced with permission.[72] Copyright 2016, WILEY-VCH. TEM image of Co_3O_4 Nanoflakes (b), Reproduced with permission.[73] Copyright 2017, ESG. TEM image of Co_3O_4 nanoplates (c), Reproduced with permission.[74] Copyright 2014, Elsevier. SEM image of Co_3O_4 nanosheets (d), Reproduced with permission.[75] Copyright 2016, WILEY-VCH. SEM image of Co_3O_4 nanosheets (e), Reproduced with permission.[76] Copyright 2016, Elsevier. SEM image of Co_3O_4 nanosheet networks (f), Reproduced with permission.[77] Copyright 2014, Elsevier. SEM image of Co_3O_4 nanosheets (g), Reproduced with permission.[78] Copyright 2018, American Chemical Society. SEM image of Co_3O_4 nanohybrids (h), Reproduced with permission.[79] Copyright 2016, Springer Nature Limited. SEM image of Co_3O_4 nanosheet arrays (i), Reproduced with permission.[80] Copyright 2018, American Chemical Society.

Besides the above mentioned 2D nanostructures that can improve the electrochemical performance of Co_3O_4-based materials, more attention is paid for nanosheets structures. Dou' group reported the atomically thin mesoporous Co_3O_4 nanosheets/graphene composites, which delivered the capacity as high as 2014.7 mAh g^{-1} at 0.1 A g^{-1} and 1134.4 mAh g^{-1} at 2.0 A g^{-1}. The distinguished electrochemical performance was ascribed to the proper thickness and the mesoporous structure of nanosheets that shortened the transportation pathway of electrons and increased the contact interfaces of electrolytes and electrodes. Meanwhile, the obtained higher capacity than theoretical specific capacity was ascribed to the pseudocapacitive contribution as the extra capacity due to unique designed layer structure, defects, edges *et al*[75] (Fig 6d). The porous Co_3O_4 nanosheets grown on the Ni foam was applied as the binder-free anode for LIBs, and delivered excellent electrochemical properties, including the high reversible capacity of 543 mAh g^{-1} even at the high current density of 20.0 A g^{-1} and cycle stability of 2000 lifespan at 5.0 A g^{-1} and 20.0 A g^{-1}[76] (Fig 6e). The electrochemical properties of 2D Co_3O_4 nanosheets were

enhanced by the 3D graphene networks, where the conductivity and the interface between electrolyte and electrode were improved and the transportation pathway was shortened, which resulted in satisfactory performance.[81] Ultra-thick mesoporous Co_3O_4 nanosheets were also grown on the Ni foam by Zhang' group, and also demonstrated desired electrochemical behaviors, which further implying the advantages of 2D nanosheets as electrodes for energy storage[77] (Fig 6f). Co_3O_4/graphene foam electrodes with good flexibility and mechanical strength were reported by Yao *et al*. The pore structure can well relieve the volume changes that keep the integrity of the electrodes during the cycling process, the nature on the electrochemical behaviors was explored, and the full cell measurements were carried out to identify the as-prepared composites[78] (Fig 6g). A Co_3O_4 hierarchical nanostructure consisting of Co_3O_4 nanoparticles and Co_3O_4 nanosheets was developed as anode electrodes and exhibited superior lithium storage behaviors[79] (Fig 6h). Li *et al*. prepared Co_3O_4 ultra-thin nanosheets to improve the kinetics of electrons and Li^+ transport of Co_3O_4-based materials and got the ideal electrochemical results[80] (Fig 6i).

3.4 Three Dimensional Co_3O_4-based Anodes

Three Dimensional (3D) nanostructures usually refer to the composites materials that are composed of one or more basic units of 0D, 1D and 2D materials. They mainly include micro-sized cages, hollow structures, mesoporous materials, flower-like structures, *etc.*[22,82-86] The 3D architecture electrodes have demonstrated excellent electrochemical performance due to good compaction, abundant mesoporous and large specific surface area.

Constructing 3D hollow structures is regarded as an effective strategy to speed up the electrochemical performance of Co_3O_4-based materials. Firstly, a hollow structure can effectively accommodate the volume changes of Co_3O_4 electrodes during the charge-discharge processes. Secondly, a hollow structure provides a large surface area, which increases the interfaces between electrodes and electrolytes and improves the number of active sites. Last but not the least, a hollow structure would shorten the diffusion pathway, offer more transportation channels for electrons and Li^+. Wang *et al*. reported multi-shelled Co_3O_4 hollow microspheres by adjusting the synthesis process parameters, which delivered satisfactory reversible capacity, rate capability and cycle performance[87] (Fig 7a). Similarly, the Co_3O_4 hollow sphere structure was constructed by Sun and his colleagues, and the as-prepared electrodes displayed an excellent capacity of 924 mAh g^{-1} at 1.0 A g^{-1}, enhanced rate capability and ultra-long cycle stability of 7000 cycles at a high current density of 5.0 A g^{-1} without obvious capacity decline[88] (Fig 7b). The porous Co_3O_4 hollow structure with adjustable porosity was prepared by a simple method of gas template-assisted spray pyrolysis, which showed excellent electrochemical performance.[96]

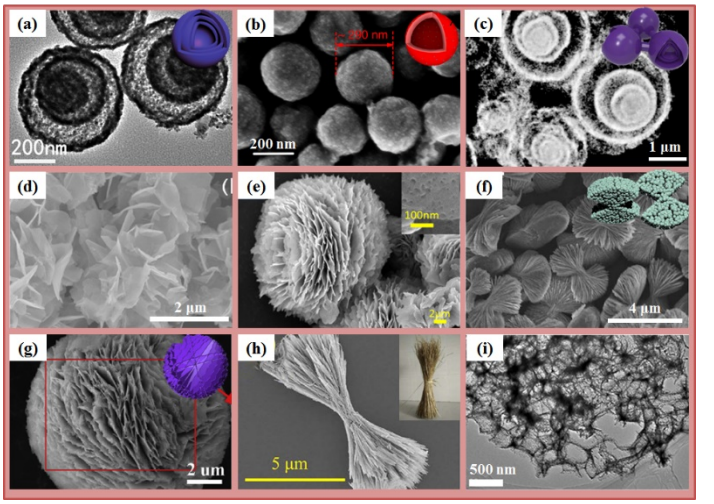

Fig. 7 3D nanostructured Co_3O_4 with different morphologies: TEM image of the multi-shelled Co_3O_4 hollow microspheres (a), Reproduced with permission.[87] Copyright 2013, Wiley-VCH. SEM image of hollow spheres (b), Reproduced with permission.[88] Copyright 2014, Macmillan Publishers Limited. TEM image of the multi-shelled Co_3O_4 hollow structure (c), Reproduced with permission.[89] Copyright 2017, Elsevier. SEM image of 3D flower-like Co_3O_4 (d), Reproduced with permission.[90] Copyright 2018, Tsinghua University Press and Springer. SEM image of flower-like Co_3O_4 (e), Reproduced with permission.[91] Copyright 2018, Springer. SEM image of bowknot-like Co_3O_4 (f), Reproduced with permission.[92] Copyright 2017, Royal Society of Chemistry. SEM image of 3D Co_3O_4 microspheres/N-doped C (g), Reproduced with permission.[93] Copyright 2018, Elsevier. SEM image of straw-sheaf-like Co_3O_4 (h), Reproduced with permission.[94] Copyright 2018, Elsevier. TEM image of 3D mesoporous network of Co_3O_4 (i), Reproduced with permission.[95] Copyright 2017, WILEY-VCH.

The uniquely designed multi-shelled Co_3O_4 hollow structure with a controllable number of internal shells was synthesized and obtained good electrochemical properties[89] (Fig 7c). In addition, the hierarchical 3D flower-like structure also plays an important role in improving the performance of Co_3O_4-based materials. Cao *et al*. reported a kind of flower-like Co_3O_4 and applied as anodes for LIBs with a desirable capacity of 920 mAh g^{-1} at 1.0 A g^{-1}, excellent rate capability and cycling behaviour[90] (Fig 7d). The 3D flower-like Co_3O_4 particles were also constructed by Zhai *et al*. and exhibited good electrochemical behaviours[91] (Fig 7e). A mesoporous bowknot-like structure was built up via hydrothermal method and heat treatment process, which displayed a high reversible capacity of 1388.8 mAh g^{-1} at 0.18 A g^{-1} after 100 cycles[92] (Fig 7f). The 3D Co_3O_4 microspheres modificated with N-doped amorphous carbon showed high reversible capacity of 830 mAh g^{-1} under a high current density of 1.0 A g^{-1} after a lifespan of 500 cycles[93] (Fig 7g). The hierarchical straw-sheaf-like Co_3O_4 was fabricated via the hydrothermal method

and the mechanism of preparation was well explored, which demonstrated superior anode electrodes properties, thanks to the unique 3D structure[94] (Fig 7h). Zhu *et al.* reported a 3D interconnected Co_3O_4 structure and the magical structure presented remarkable lithium storage performance[95] (Fig 7i). In our group, we manufactured mesoporous hollow Co_3O_4 microspheres via a facial two-step hydrothermal strategy and introduced oxygen vacancies into the structure by the heat treatment process (Fig. 8).[97] The delivered outstanding electrochemical performance of the prepared samples can be explained by the concept of local built-in electric field, which caused by the unbalanced charge distribution around the oxygen vacancy region, promoting the Li^+ intercalation/deintercalation process. This strategy cast light on developing Co_3O_4 and other transition metal oxides as anode electrodes for LIBs.[98]

Furthermore, 3D Co_3O_4 cube structures have been developed to improve electrochemical performance. Micro-/nanostructured Co_3O_4 cube structures were synthesized by Huang *et al.* and the electrode with such unique morphology showed a high capacity and capacity retention.[99] Deng *et al.* reported a Co_3O_4-based composite that Co_3O_4 nanoparticles were covered with double carbon coating of 3D porous carbon network and cubic N-doping carbon shell. The as-prepared electrodes presented outstanding electrochemical performance of 1208 mAh g^{-1} at 0.1 A g^{-1} after 100 cycles, excellent rate capability of 539 mAh g^{-1} at 10.0 A g^{-1}, and 516 mAh g^{-1} under 5.0 A g^{-1} for 400 cycles due to the merits of structure, including high porosity, high surface area, high conductivity and physical stability.[100] The cubic Co_3O_4 composites structure was also constructed by Wang's group, where the Co_3O_4 nanoparticles were dispersed in the cubic hierarchically porous carbon matrix, delivered prominent capacity property.[32] The metal-organic framework-derived Co_3O_4 particles were protected by MoS_2 nanosheets, which accommodated the volume changes during the charge-discharge process, resulting in remarkable lithium storage properties.[101] Meanwhile, Lou's group prepared multishelled Co_3O_4@$Co_3V_2O_8$ nanoboxes, and showed satisfactory electrochemical characteristics.[102]

4. Conclusions and Perspectives

With the huge demands for energy storage devices, especially for lithium ion batteries with outstanding performance, electrode materials with even higher energy and power densities will continue to be developed. Co_3O_4-based materials, traditional transition metal oxides, are still charming as anode electrodes for LIBs due to the huge potential for the next generation anodes to meet the requirements of high performance.

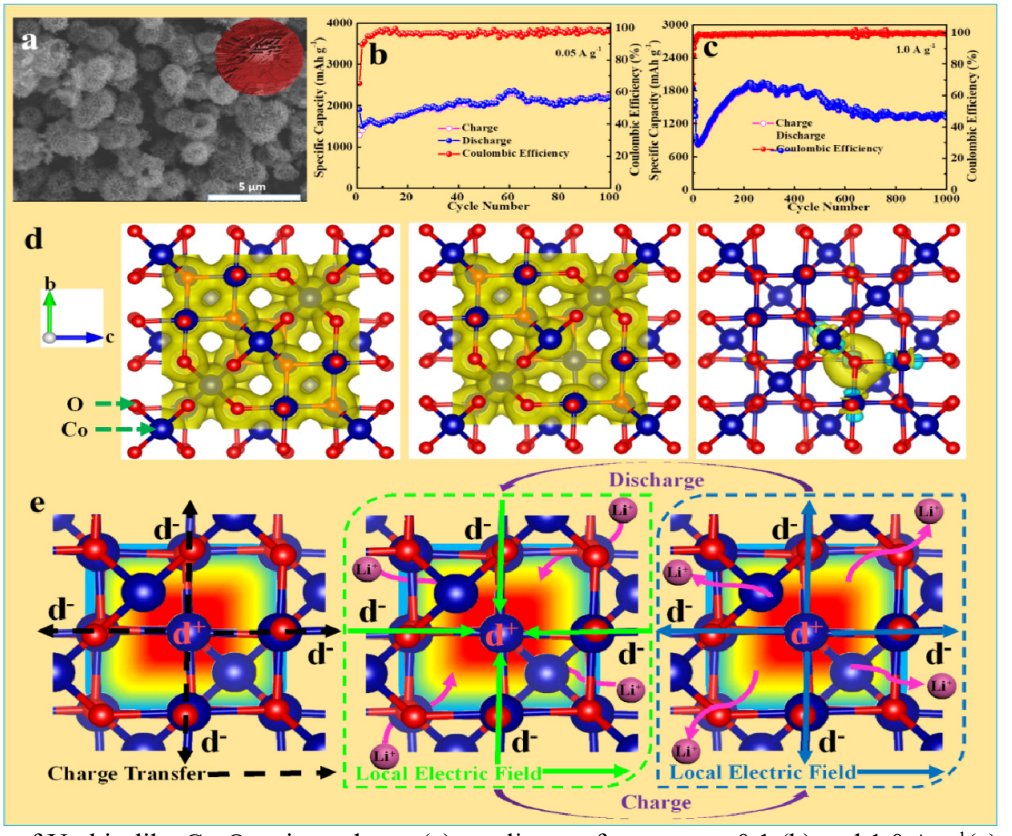

Fig. 8 SEM image of Urchin-like Co_3O_4 microspheres (a), cycling performance at 0.1 (b) and 1.0 A g^{-1}(c) and the schematic illustration of the mechanism of local built-in electric field caused by oxygen vacancies. Reproduced with permission.[98] Copyright 2018, Royal Society of Chemistry.

In this work, we have summarized the recent developments in high performance Co_3O_4 and the composites as anode materials for LIBs. The morphology and electrochemical performance are discussed through different dimensions, including 0D (nanospheres, nanocrystals, nanoparticles, nanocages and nanocubes), 1D (nanowires, nanofibers, nanorods and nanotubes), 2D (nanosheets, nanofoils, nanoflakes and films) and 3D structures (microsized cages, hollow structures, mesoporous materials, flower-like structures). Since Co_3O_4-based materials are faced with low electrical conductivity and huge volume expansion during charge-discharge processes, which hinder the commercial application. Different strategies have been applied to overcome these drawbacks. The preparation of the nanosized particles (various nanostructures), introducing conductive carbon matrix (carbon nanofibers, graphene, carbon nanotubes, N-doping porous amorphous carbon *et al.*), constructing special structures (hollow structure, flower-like structures, mesoporous materials, core-shell structure *et al.*) have been proved to be effective in improving the electrochemical performance of Co_3O_4-based materials. With the unique designed nanostructure, the practical application of Co_3O_4-based electrodes with the enhanced electrochemical performance for next-generation LIBs may be realized in the near future, and the development will be promoted by the emerging machine-learning techniques.

To fit the practical application, the lithium storage properties of Co_3O_4-based electrodes, including rate capability and stable long-lifespan still have plenty of room to enhance. In order to better meet the needs of commercial applications of Co_3O_4-based electrodes for LIBs, the facial, inexpensive, environmentally friendly, and mass-producible methods are needed to be developed. Meanwhile, the size and morphology of Co_3O_4-based electrodes, especially the microsized and uniform particles that are more conducive to large-scale production, need to be controlled strictly. In addition, the understanding of the mechanisms behind the performance and the materials' formation play an important role in unraveling the improved electrochemical performance, which will provide the guideline to design new materials for energy storage electrodes.

Acknowledgements

This work was supported by research program of the Key Laboratory of Biomedical Effects of Nanomaterials and Nanosafety, Chinese Academy of Sciences (No: NSKF201908) and the research program of Top Discipline in Materials Science of Shandong Province.

Conflict of interest

There are no conflicts to declare.

Supporting information

Not applicable.

References

[1] C. Li, S. Dong, P. Wang, C. Wang and L. Yin, *Adv. Energy Mater.*, 2019, **9**, 1902352, doi: 10.1002/aenm.201902352.

[2] C. Li, S. Dong, R. Tang, X. Ge, Z. Zhang, C. Wang, Y. Lu and L. Yin, *Energy Environ. Sci.*, 2018, **11**, 3201-3211, doi: 10.1039/c8ee01046c.

[3] J. Guan, H. Xiao, X. Lou, Y. Guo, X. Luo, Y. Li, C. Yan, X. Yan, G. Gao, H. Yuan, J. Dai, R. Su, W. Gu and Z. Guo, *ES Energy Environ.*, 2018, **1**, 80-88, doi: 10.30919/esee8c126.

[4] L. Yan, H. Wang, D. Huang and H. Luo, *Eng. Sci.*, 2018, **1**, 4-20, doi: 10.30919/es.180318.

[5] W. Du, X. Wang, J. Zhan, X. Sun, L. Kang, F. Jiang, X. Zhang, Q. Shao, M. Dong, H. Liu, V. Murugadoss and Z. Guo, *Electrochim. Acta*, 2019, **296**, 907-915, doi: 10.1016/j.electacta.2018.11.074.

[6] S. Li, C. Yang, S. Sarwar, A. Nautiyal, P. Zhang, H. Du, N. Liu, J. Yin, K. Deng and X. Zhang, *Adv. Compos. Hybrid Mater.*, 2019, **2**, 279-288, doi: 10.1007/s42114-019-00103-w.

[7] Y. Fu, X. Pei, Y. Dai, D. Mo and S. Lyu, *ES Energy Environ.*, 2019, **4**, 66-73, doi: 10.30919/esee8c292.

[8] X. Zhang, X. Li, F. Jiang, W. Du, C. X. Hou, Z. Xu, L. Zhu, Z. Wang, H. Liu, W. Zhou and H. Yuan, *Dalton T.*, 2020, **49**, 1794-1802, doi: 10.1039/c9dt03845k.

[9] Y. Yao, J. Zheng, Z. Gong, Z. Ding, J. Zhang, W. Yu, D. A. M. Bengono, H. Li, B. Zhang and H. Tong, *J. Alloy. Compd.*, 2019, **790**, 288-295, doi: 10.1016/j.jallcom.2019.03.098.

[10] R. Li, C. Lin, N. Wang, L. Luo, Y. Chen, J. Li and Z. Guo, *Adv. Compos. Hybrid Mater.*, 2018, **1**, 440-459, doi: 10.1007/s42114-018-0038-1.

[11] H. Tong, Q. Zhou, B. Zhang, X. Wang, Y. Yao, Z. Ding, H. Chen, J. Zheng and W. Yu, *Eng. Sci.*, 2019, **8**, 25-32, doi: 10.30919/es8d502.

[12] A. Kraytsberg and Y. Ein-Eli, *Adv. Energy Mater.*, 2012, **2**, 922-939, doi: 10.1002/aenm.201200068.

[13] Y. Zhang, Y. Li, X. Xia, X. Wang, C. Gu and J. Tu, *Sci. China Technol. Sci.*, 2015, **58**, 1809-1828, doi: 10.1007/s11431-015-5933-x.

[14] Y. Chu, L. Guo, B. Xi, Z. Feng, F. Wu, Y. Lin, J. Liu, D. Sun, J. Feng, Y. Qian and S. Xiong, *Adv. Mater.,* 2018, **30**, 1704244, doi: 10.1002/adma.201704244.

[15] M. Idrees, L. Liu, S. Batool, H. Luo, J. Liang, B. Xu, S. Wang and J. Kong, *Eng. Sci.*, 2019, **6**, 64-76, doi: 10.30919/es8d798.

[16] M. S. Balogun, W. Qiu, Y. Luo, H. Meng, W. Mai, A. Onasanya, T. K. Olaniyi and Y. Tong, *Nano Res.*, 2016, **9**, 2823-2851, doi: 10.1007/s12274-016-1171-1.

[17] J. Lu, Z. Chen, F. Pan, Y. Cui and K. Amine, *Electrochem. Energy Rev.*, 2018, **1**, 35-53, doi: 10.1007/s41918-018-0001-4.

[18] S. Goriparti, E. Miele, F. De Angelis, E. Di Fabrizio, R. Proietti Zaccaria and C. Capiglia, *J. Power Sources*, 2014, **257**, 421-443, doi: 10.1016/j.jpowsour.2013.11.103.

[19] W. Li, X. Sun and Y. Yu, *Small Methods*, 2017, **1**, 1600037, doi: 10.1002/smtd.201600037.

[20] Y. Han, J. Zou, Z. Li, W. Wang, Y. Jie, J. Ma, B. Tang, Q. Zhang, X. Cao, S. Xu and Z. L. Wang, *ACS Nano*, 2018, **12**, 4835-4843, doi: 10.1021/acsnano.8b01558.
[21] C. Hou, Z. Tai, L. Zhao, Y. Zhai, Y. Hou, Y. Fan, F. Dang, J. Wang and H. Liu, *J. Mater. Chem. A*, 2018, **6**, 9723-9736, doi: 10.1039/c8ta02863j.
[22] C. Hou, J. Wang, W. Du, J. Wang, Y. Du, C. Liu, J. Zhang, H. Hou, F. Dang, L. Zhao and Z. Guo, *J. Mater. Chem. A*, 2019, **7**, 13460-13472, doi: 10.1039/c9ta03551f.
[23] Z. Zhang, L. Gao, Y. Dong, J. Zhao and Z. Wu, *Prog. Nat. Sci. Mater. Int.*, 2018, **28**, 212-217, doi: 10.1016/j.pnsc.2018.02.005.
[24] P. Poizot, S. Laruelle, S. Grugeon, L. Dupont and J. M. Tarascon, *J. Power Sources*, 2001, **97-98**, 235-239, doi: 10.1016/S0378-7753(01)00508-0.
[25] M. Xu, Q. Xia, J. Yue, X. Zhu, Q. Guo, J. Zhu and H. Xia, *Adv. Funct. Mater.*, 2018, **29**, 1807377, doi: 10.1002/adfm.201807377.
[26] Y. Tian, X. Yang, A. Nautiyal, Y. Zheng, Q. Guo, J. Luo and X. Zhang, *Adv. Compos. Hybrid Mater.*, 2019, **2**, 151-161, doi: 10.1007/s42114-019-0075-4.
[27] Q. Wang, J. Zhang, Z. Zhang, Y. Hao and K. Bi, *Adv. Compos. Hybrid Mater.*, 2020, **3**, 58-65, doi: 10.1007/s42114-020-00138-4.
[28] N. Yan, L. Hu, Y. Li, Y. Wang, H. Zhong, X. Hu, X. Kong and Q. Chen, *J. Phys. Chem. C*, 2012, **116**, 7227-7235, doi: 10.1021/jp2126009.
[29] K. Xiao, L. Zhang, Q. Tang, B. Fan, A. Hu, S. Zhang, W. Deng and X. Chen, *J. Solid State Electrochem.*, 2018, **22**, 2321-2328, doi: 10.1007/s10008-018-3928-9.
[30] J. Y. Cheong, J. H. Chang, S. H. Cho, J. W. Jung, C. Kim, K. S. Dae, J. M. Yuk and I. D. Kim, *Electrochim. Acta*, 2019, **295**, 7-13, doi: 10.1016/j.electacta.2018.10.080.
[31] Y. Chen, Y. Wang, Z. Wang, M. Zou, H. Zhang, W. Zhao, M. Yousaf, L. Yang, A. Cao and R. P. S. Han, *Adv. Energy Mater.*, 2018, **8**, 1702981, doi: 10.1002/aenm.201702981.
[32] Y. Fu, Y. Li, R. Zhou, Y. Zhang, S. Chen, Y. Song and L. Wang, *J. Alloy. Compd.*, 2018, **749**, 645-651, doi: 10.1016/j.jallcom.2018.03.338.
[33] K. Jang, D. K. Hwangb, F. M. Auxilia, J. Jang, H. Song, B. Y. Oh, Y. Kim, J. Nam, J. W. Park, S. Jeong, S. S. Lee, S. Choi, In S. Kim, W. B. Kim, J. M. Myoung and M. H. Hama, *Chem. Eng. J.*, 2017, **309**, 15-21, doi: 10.1016/j.cej.2016.10.009.
[34] H. H. Li, L. Zhou, L. L. Zhang, C. Y. Fan, H. H. Fan, X. L. Wu, H. Z. Sun and J. P. Zhang, *ACS Energy Lett.*, 2016, **2**, 52-59, doi: 10.1021/acsenergylett.6b00564.
[35] Y. Yang, J. Huang, J. Zeng, J. Xiong and J. Zhao, *ACS Appl. Mater. Interf.*, 2017, **9**, 32801-32811, doi: 10.1021/acsami.7b10683.
[36] K. Zhou, L. Lai, Y. Zhen, Z. Hong, J. Guo and Z. Huang, *Chem. Eng. J.*, 2017, **316**, 137-145, doi: 10.1016/j.cej.2017.01.060.
[37] D. Wang, Y. Yu, H. He, J. Wang, W. Zhou and H. D. Abruna, *ACS Nano*, 2015, **9**, 1775-1781, doi: 10.1021/nn506624g.
[38] Y. M. Chen, L.Yu and X. W. Lou, *Angew. Chem. Int. Ed.*, 2016, **55**, 5990-5993, doi: 10.1002/anie.201600133.
[39] F. Ran, X. Yang and L. Shao, *Adv.Compos. Hybrid Mater.,* 2018, **1**, 32-55, doi: 10.1007/s42114-017-0021-2.
[40] T. Kesavan, N. Gunawardhana, C. Senthil, M. Kundu, G. Maduraiveeran, M. Yoshio and M. Sasidharan, *Chemistry Select*, 2018, **3**, 5502-5511, doi: 10.1002/slct.201800445.
[41] Y. Zhao, L. P. Wang, M. T. Sougrati, Z. Feng, Y. Leconte, A. Fisher, M. Srinivasan and Z. Xu, *Adv. Energy Mater.*, 2017, **7**, 1601424, doi: 10.1002/aenm.201601424.
[42] G. Huang, F. Zhang, X. Du, Y. Qin, D. Yin and L. Wang, *ACS Nano*, 2015, **9**, 1592-1599, doi: 10.1021/nn506252u.
[43] M. Xu, F. Wang, Y. Zhang, S. Yang, M. Zhao and X. Song, *Nanoscale*, 2013, **5**, 8067-8072, doi: 10.1039/c3nr02538a.
[44] Z. Yan, Q. Hu, G. Yan, H. Li, K. Shih, Z. Yang, X. Li, Z. Wang and J. Wang, *Chem. Eng. J.*, 2017, **321**, 495-501, doi: 10.1016/j.cej.2017.03.146.
[45] M. Zhong, W. W. He, W. Shuang, Y. Y. Liu, T. L. Hu and X. H. Bu, *Inorg. Chem.*, 2018, **57**, 4620-4628, doi: 10.1021/acs.inorgchem.8b00365.
[46] Hou, G. Liu, F. Dang, Z. Zhang and J. Chen, *Journal of Wuhan University of Technology-Mater. Sci. Ed.*, 2017, **32**, 871-874, doi: 10.1007/s11595-017-1682-y.
[47] C. Cheng, Y. Jiang, X. Sun, J. Shen, T. Wang, G. Fan and R. Fan, *Compos Part A Appl. Sci. Manufac.*, 2020, **130**, 105753, doi: 10.1016/j.compositesa.2019.105753.
[48] Y. Li, X. Wang, Z. Wang and L. Chen, *ES Energy Environ.*, 2019, **3**, 55-59, doi: 10.30919/esee8c198.
[49] R. Nie, Q. Wang, P. Sun, R. Wang, Q. Yuan and X. Wang, *Eng. Sci.*, 2019, **6**, 22-29, doi: 10.30919/es8d668.
[50] Q. Zhang, J. Dai, M. Liao, T. Duan and W. Yao, *Eng. Sci.*, 2019, **7**, 43-51, doi: 10.30919/es8d728.
[51] S. M. Aqeel, Z. Huang, J. Walton, C. Baker, D. Falkner, Z. Liu and Z. Wang, *Adv. Compos. Hybrid Mater.*, 2018, **1**, 185-192, doi: 10.1007/s42114-017-0002-5.
[52] D. Gu, W. Li, F. Wang, H. Bongard, B. Spliethoff, W. Schmidt, C. Weidenthaler, Y. Xia, D. Zhao and F. Schuth, *Angew. Chem. Int. Ed.*, 2015, **54**, 7060-7064, doi: 10.1002/anie.201501475.
[53] Y. Chen, Y. Wang, H. Yang, H. Gan, X. Cai, X. Guo, B. Xu, M. Lü and A. Yuan, *Ceram. Int.*, 2017, **43**, 9945-9950, doi: 10.1016/j.ceramint.2017.05.004.
[54] C. L. Zhang, B. R. Lu, F. H. Cao, Z. L. Yu, H. P. Cong and S. H. Yu, *J. Mater. Chem. A*, 2018, **6**, 12962-12968, doi: 10.1039/c8ta03397h.
[55] L. Fan, W. Zhang, S. Zhu and Y. Lu, *Ind. Eng. Chem. Res.*, 2017, **56**, 2046-2053, doi: 10.1021/acs.iecr.7b00222.
[56] C. Yan, G. Chen, X. Zhou, J. Sun and C. Lv, *Adv. Funct. Mater.*, 2016, **26**, 1428-1436, doi: 10.1002/adfm.201504695.
[57] Y. Tan, Q. Gao, Z. Li, W. Tian, W. Qian, C. Yang and H. Zhang, *Sci. Rep.*, 2016, **6**, 26460, doi: 10.1038/srep26460.

[58] Tong, M. Zeng, J. Li and Z. Liu, *J. Alloy. Compd.*, 2017, **723**, 129-138, doi: 10.1016/j.jallcom.2017.06.209.
[59] H. Wang, S. Zhuo, Y. Liang, X. Han and B. Zhang, *Angew. Chem. Int. Ed.*, 2016, **55**, 9055-9059, doi: 10.1002/anie.201603197.
[60] C. Yan, Y. Zhu, Y. Li, Z. Fang, L. Peng, X. Zhou, G. Chen and G. Yu, *Adv. Funct. Mater.,* 2018, **28**, 1705951, doi: 10.1002/adfm.201705951.
[61] X. Li, X. Tian, T. Yang, Y. Song and Z. Liu, *Chemistry*, 2018, **24**, 14477-14483, doi: 10.1002/chem.201802715.
[62] Y. Ma, J. He, Z. Kou, A. M. Elshahawy, Y. Hu, C. Guan, X. Li and J. Wang, *Adv. Mater. Interf.*, 2018, **5**, 1800222, doi: 10.1002/admi.201800222.
[63] H. Wu, M. Xu, Y. Wang and G. Zheng, *Nano Res.*, 2013, **6**, 167-173, doi: 10.1007/s12274-013-0292-z.
[64] H. Gao, H. Sun, A. Zhao, L. Wang and N. Liu, *Int. J. Electrochem. Sci.*, 2018, **13**, 8666-8672, doi: 10.20964/2018.09.18.
[65] X. Yang, K. Fan, Y. Zhu, J. Shen, X. Jiang, P. Zhao, S. Luan and C. Li, *ACS Appl. Mater. Interf.*, 2013, **5**, 997-1002, doi: 10.1021/am302685t.
[66] K. M. Shaju, F. Jiao, A. Debart and P. G. Bruce, *Phys. Chem. Chem. Phys.*, 2007, **9**, 1837-1842, doi: 10.1039/b617519h.
[67] C. Hou, T. Liu, Y. Fan, H. Imai, R. Fan, H. Lin, Q. He, N. Wang, F. Dang and Z. Guo, *CrystEngComm*, 2016, **18**, 3008-3014, doi: 10.1039/c6ce00282j.
[68] Y. Hou, C. Hou, Y. Fan, F. Dang and B. W. Li, *Mater. Res. Express*, 2017, **4**, 125028, doi: 10.1088/2053-1591/aa9e65.
[69] K. Sun, J. Dong, Z. Wang, Z. Wang, G. Fan, Q. Hou, L. An, M. Dong, R. Fan and Z. Guo, *J. Phys. Chem. C*, 2019, **123**, 23635-23642, doi: 10.1021/acs.jpcc.9b06753.
[70] L. Sun, Z. Shi, H. Wang, K. Zhang, D. Dastan, K. Sun and R. Fan, *J. Mater. Chem. A*, 2020, **8**, 5750-5757, doi: 10.1039/d0ta00903b.
[71] G. Zhao, L. Tang, L. Zhang, X. Chen, Y. Mao and K. Sun, *J. Alloy. Compd.*, 2018, **746**, 277-284, doi: 10.1016/j.jallcom.2018.02.285.
[72] W. Eom, A. Kim, H. Park, H. Kim and T. H. Han, *Adv. Funct. Mater.*, 2016, **26**, 7605-7613, doi: 10.1002/adfm.201602320.
[73] V. Nulu, A. Nulu and K.Yong Sohn, *Int. J. Electrochem. Sci.*, 2018, **13**, 2069-2079, doi: 10.20964/2018.02.73.
[74] Q. Su, J. Zhang, Y. Wu and G. Du, *Nano Energy*, 2014, **9**, 264-272, doi: 10.1016/j.nanoen.2014.08.006.
[75] Y. Dou, J. Xu, B. Ruan, Q. Liu, Y. Pan, Z. Sun and S. X. Dou, *Adv. Energy Mater.*, 2016, **6**, 1501835, doi: 10.1002/aenm.201501835.
[76] G. Fang, J. Zhou, C. Liang, A. Pan, C. Zhang, Y. Tang, X. Tan, J. Liu and S. Liang, *Nano Energy*, 2016, **26**, 57-65, doi: 10.1016/j.nanoen.2016.05.009.
[77] X. Wang, Y. Fan, R. A. Susantyoko, Q. Xiao, L. Sun, D. He and Q. Zhang, *Nano Energy*, 2014, **5**, 91-96, doi: 10.1016/j.nanoen.2014.02.005.
[78] Y. Yao, Y. Zhu, S. Zhao, J. Shen, X. Yang and C. Li, *ACS Appl. Energy Mater.*, 2018, **1**, 1239-1251, doi: 10.1021/acsaem.7b00351.
[79] J. Mujtaba, H. Sun, G. Huang, K. Molhave, Y. Liu, Y. Zhao, X. Wang, S. Xu and J. Zhu, *Sci. Rep.*, 2016, **6**, 20592, doi: 10.1038/srep20592.
[80] J. Li, Z. Li, F. Ning, L. Zhou, R. Zhang, M. Shao and M. Wei, *ACS Omega*, 2018, **3**, 1675-1683, doi: 10.1021/acsomega.7b01832.
[81] H. Sun, Y. Liu, Y. Yu, M. Ahmad, D. Nan and J. Zhu, *Electrochim. Acta*, 2014, **118**, 1-9, doi: 10.1016/j.electacta.2013.11.181.
[82] Y. Wang, Y. Liu, C. Wang, H. Liu, J. Zhang, J. Lin, J. Fan, T. Ding, J. E. Ryu and Z. Guo, *Eng. Sci.*, 2020, **9**, 50-59, doi: 10.30919/es8d903.
[83] C. Hou, Y. Oaki, E. Hosono, H. Lin, H. Imai, Y. Fan and F. Dang, *Mater. Design*, 2016, **109**, 718-725, doi: 10.1016/j.matdes.2016.07.099.
[84] C. Hou, J. Wang, W. Zhang, J. Li, R. Zhang, J. Zhou, Y. Fan, D. Li, F. Dang, J. Liu, Y. Li, K. Liang and B. Kong, *ACS Appl. Mater. Interf.*, 2020, **12**, 13770-13780, doi: 10.1021/acsami.9b20317.
[85] Y. Lv, L. Zhu, H. Xu, L. Yang, Z. Liu, D. Cheng, X. Cao, J. Yun and D. Cao, *Eng. Sci.*, 2019, **7**, 26-37, doi: 10.30919/es8d768.
[86] X. Wang, X. Zeng and D. Cao, *Eng. Sci.*, 2018, **1**, 55-63, doi: 10.30919/es.180325.
[87] J. Wang, N. Yang, H. Tang, Z. Dong, Q. Jin, M. Yang, D. Kisailus, H. Zhao, Z. Tang and D. Wang, *Angew. Chem. Int. Ed.*, 2013, **52**, 6417-6420, doi: 10.1002/anie.201301622.
[88] H. Sun, G. Xin, T. Hu, M. Yu, D. Shao, X. Sun and J. Lian, *Nat. Commun.*, 2014, **5**, 4526, doi: 10.1038/ncomms5526.
[89] Z. Wang, S. Qu, Y. Cheng, C. Zheng, S. Chen and H. Wu, *Appl. Surf. Sci.*, 2017, **416**, 338-343, doi: 10.1016/j.apsusc.2017.04.194.
[90] W. Cao, W. Wang, H. Shi, J. Wang, M. Cao, Y. Liang and M. Zhu, *Nano Res.*, 2018, **11**, 1437-1446, doi: 10.1007/s12274-017-1759-0.
[91] X. Zhai, X. Xu, X. Zhu, Y. Zhao, J. Li and H. Jin, *J. Mater. Sci.*, 2018, **53**, 1356-1364, doi: 10.1007/s10853-017-1579-3.
[92] H. Du, C. Yuan, K. Huang, W. Wang, K. Zhang and B. Geng, *J. Mater. Chem. A*, 2017, **5**, 5342-5350, doi: 10.1039/c6ta10327h.
[93] M. Liu, X. Hou, T. Wang, Y. Ma, K. Sun, D. Liu, Y. Wang, D. He and J. Li, *Electrochim. Acta*, 2018, **283**, 979-986, doi: 10.1016/j.electacta.2018.07.021.
[94] B. Wang, X. Y. Lu, C. W. Tsang, Y. Wang, W. K. Au, H. Guo and Y. Tang, *Chem. Eng. J.*, 2018, **338**, 278-286, doi: 10.1016/j.cej.2017.12.124.
[95] S. Zhu, J. Li, X. Deng, C. He, E. Liu, F. He, C. Shi and N. Zhao, *Adv. Funct. Mater.*, 2017, **27**, 1605017, doi: 10.1002/adfm.201605017.

[96] H. Du, K. Huang, M. Li, Y. Xia, Y. Sun, M. Yu and B. Geng, *Nano Res.*, 2018, **11**, 1490-1499, doi: 10.1007/s12274-017-1766-1.
[97] Y. Hou, C. Hou, Y. Zhai, H. Li, T. Chen, Y. Fan, H. Wang and W. Wang, *Electrochim. Acta*, 2019, **324**, 134884, doi: 10.1016/j.electacta.2019.134884.
[98] C. Hou, Y. Hou, Y. Fan, Y. Zhai, Y. Wang, Z. Sun, R. Fan, F. Dang and J. Wang, *J. Mater. Chem. A*, 2018, **6**, 6967-6976, doi: 10.1039/c8ta00975a.
[99] G. Huang, S. Xu, S. Lu, L. Li and H. Sun, *ACS Appl. Mater. Interf.*, 2014, **6**, 7236-7243, doi: 10.1021/am500452t.
[100] X. Deng, S. Zhu, F. He, E. Liu, C. He, C. Shi, Q. Li, J. Li, L. Ma and N. Zhao, *Electrochim. Acta*, 2018, **283**, 1269-1276, doi: 10.1016/j.electacta.2018.07.061.
[101] J. Wang, H. Zhou, M. Zhu, A. Yuan and X. Shen, *J. Alloy. Compd.*, 2018, **744**, 220-227, doi: 10.1016/j.jallcom.2018.02.086.
[102] Y. Lu, L. Yu, M. Wu, Y. Wang and X. W. D. Lou, *Adv. Mater.*, 2018, **30**, 1702875, doi: 10.1002/adma.201702875.

